MDPI

Article

Effects of Ultrasonic Pretreatment on the Discharge for Better Recycling of Spent Lithium-Ion Batteries

Weichen Yang [1], Zheng Tong [1], Hezhan Wan [1], Shuangyin Jiang [1], Xiangning Bu [1,*] and Lisha Dong [2,*]

[1] Key Laboratory of Coal Processing and Efficient Utilization (Ministry of Education), School of Chemical Engineering and Technology, China University of Mining and Technology, Xuzhou 221116, China
[2] Western Australian School of Mines: Minerals, Energy and Chemical Engineering, Curtin University, Kalgoorlie, WA 6430, Australia
* Correspondence: xiangning.bu@cumt.edu.cn (X.B.); lisha.dong@curtin.edu.au (L.D.)

Abstract: Discharge treatment is a vital process in the pretreatment of spent lithium-ion batteries (LIBs). This paper focuses on the effects of ultrasonic pretreatment on the discharge of spent LIBs from the perspective of electrolyte concentration and ultrasonic power. By integrating characterizations such as pH measurement and X-ray fluorescence (XRF), the effect of ultrasonic pretreatment on the discharge of spent LIBs is evaluated. Experimental results show that sodium chloride (NaCl) solution and potassium chloride (KCl) solution have a more significant and better discharge efficiency (*DE*) under ultrasonic treatment, while organic electrolyte solutions which mainly contain formate and acetate generally show a less ideal *DE*. Under experimental conditions of using electrolyte discharge solutions with various electrolyte concentrations with the same ultrasonic power of 300 W, the *DE* generated from the experimental condition with KCl solution in 30 g/200 mL deionized water is the highest, 64.9%; under different ultrasonic powers in the same electrolyte solutions, the *DE* of 10 wt.% HCOONa solution is the highest at ultrasonic power of 500 W, at 4.7%. This work provides a reference for the efficient and cost-effective pretreatment of spent LIBs and the discharge mechanism in different electrolyte solutions with ultrasonic treatment is also explored to support the recycling of spent LIBs.

Keywords: ultrasonic pretreatment; discharge; spent lithium-ion battery

1. Introduction

Material separation poses a significant technical challenge to recycling efficiency (*DE*), particularly due to the heterogeneous and complex nature of most spent lithium-ion battery (LIB) streams. Sorting, discharging, disassembly, and pretreatment processes are generally described as cumbersome and impractical by stakeholders, thus, it was suggested that discharge triggers and design-for-disposal principles should be considered by battery manufacturers to enhance the safety and efficiency of disassembly and recycling processes [1].

In the past two decades, researchers have published many review articles on the recycling of spent LIBs. These papers systematically review the current research status, existing challenges, and future development trends of spent LIB recycling processes at both laboratory and industrial scales. The analysis is conducted from a multidimensional perspective, considering economic, technological, and environmental factors [2–13]. The resource recycling of spent LIBs mainly includes preprocessing (discharging, dismantling, crushing, sorting, and preliminary separation of electrode materials) [14–22], metallurgical recycling (hydrometallurgical and pyrometallurgical techniques to improve the grade of

valuable metals) [23,24], and regeneration of electrode materials [19,25,26]. Discharge treatment is a very critical part of the pretreatment of spent LIBs. The high voltage remaining in spent LIBs is not conducive to the implementation of resource recycling, and the hazards are mainly fires and explosions caused by unnecessary short circuits [27–29]. In addition, the high voltage and reactive components of spent LIBs pose safety risks during the mechanical processing and crushing stages, as well as storage and transportation [30]. The selection of *DE* and mode is a very basic but critical step in the spent LIB recycling process. The discharge methods for spent LIB pretreatment include physical discharge, chemical discharge, and low-temperature freezing discharge [31,32]. Physical discharge is a method of discharging the spent battery by connecting a load at both ends of the electrodes to consume the remaining energy below the safe voltage. Voltage rebound and false discharge may occur during physical discharge, leaving a significant amount of residual energy in spent batteries, which poses potential risks to subsequent recycling processes [33]. Su et al. [33] carried out research on the safe discharge of spent LIBs, and different physical discharge methods were studied. It was found that energy-saving feedback discharge, electronic load discharge, and conductor powder discharge had voltage rebound, local overheating, and false discharge, making it difficult to achieve large-scale applications of spent LIB discharge. Low-temperature freezing discharge is a method of discharging batteries under low-temperature conditions. This discharge method demands highly specialized equipment and incurs significant costs, making it unsuitable for large-scale batch processing of spent LIBs [34].

Chemical discharge is the electrochemical reaction of LIBs as a power source in various electrolyte solutions [33], and common electrolyte solutions are mainly based on sulfates, chlorides, etc. Fang et al. [35] conducted discharge experiments on spent 18650 cylindrical LIBs in different electrolyte solutions. The residual voltage of the spent battery was effectively consumed in 0.8 mol/L NaCl solution, and the *DE* was high. However, the battery shell was severely corroded in the NaCl solution, resulting in electrolyte leakage and environmental pollution. Chen et al. [31] used the same 18650 type of spent LIBs, and different electrolyte solutions were tested for chemical discharge to pretreat the spent LIBs. The KCl solution can also effectively consume the battery's residual voltage. Su et al. [36] carried out chemical discharge experiments and found that there was no Na_2SO_4 loss during the discharge, and the highest *DE* was generated from the experiment with a 50% saturated Na_2SO_4 solution. Torabian et al. [29] discharged spent LIBs with 16% NaCl solution under ultrasonic-assisted conditions and found that the *DE* could be significantly improved under the ultrasonic treatment with an ultrasound power of 50 W. Compared with physical discharge and low-temperature freezing discharge, chemical discharge is easy to operate and does not cause voltage rebound and overheating. Therefore, it is safer and more suitable for large-scale discharge of spent LIBs. It is widely used in the pretreatment of industrial spent LIBs [37]. However, chemical discharge may cause corrosion to the battery casing and lead to battery electrolyte leakage, causing environmental pollution.

In this work, NaCl, KCl, Na_2SO_4, HCOONa, CH_3COONa, and $(CH_3COO)_2Zn$ solutions were used under ultrasonic-assisted conditions to explore the effects of electrolyte concentration and ultrasonic power on battery *DE* and corrosion. Various characterizations of products are carried out, such as pH measurement and X-ray fluorescence (XRF), to comprehensively assess the changes in electrolyte solutions and the formation of discharge by-products during the discharge. By integrating these characterizations, a comprehensive evaluation of the impacts of ultrasonic pretreatment on the *DE* wasconducted, shedding light on the underlying mechanisms. This study enhances our understanding and offers valuable insights for optimizing the LIB recycling process, ultimately advancing greener and more efficient chemical discharge methods.

2. Materials and Methodology

2.1. Materials

NaCl (AR, ≥99.5%), KCl (AR, ≥99.5%) and anhydrous Na_2SO_4 (AR, ≥99.0%) are purchased from Xilong Scientific, while NaCOOH (AR, ≥99.0%), anhydrous CH_3COONa (AR, ≥99.0%), and anhydrous $(CH_3COO)_2Zn$ (AR, ≥98.0) are purchased from Sinopharm Chemical Reagent.

2.2. Experimental Apparatus and Devices

2.2.1. Experimental Apparatus

The experimental apparatus used in this work and working conditions are listed in Table 1.

Table 1. Equipment used in the present work and their working conditions.

Experimental Facilities	Model and Working Condition	Manufacturer
BAK disassembled battery	BAK 18650-2150 Mah battery with an initial voltage of 3.8 V	BAK from car teardown
Wires	Oxygen-free Cu core and PVC sheath, and loading voltage of 300 V	Generic
99.6% pure nickel	99.6% pure nickel (0.5 mm × 15 mm per meter) 0.5 mm in thickness, 15 mm in width	Quanzhou Baiyixing Electronic Technology
Digital multifunction electricity meter	VC890C+	Xi'an Beicheng Electronics
Circulating water vacuum pump	SHZ-D III	Yuhua Brand
Ultrasonic cleaning equipment	AK-080SD	Yuclean
Plastic centrifuge tubes, beakers, rubber droppers, and battery boxes	N/A	Generic

2.2.2. Preparation for XRF Analysis

Innitially, 5 g samples with a particle size of ≤200 mesh (~75 μm) were collected and made into tablets with boric acid. All the experiments were carried out in a standard analytical laboratory at room temperature.

2.3. Effects of Electrolyte Concentration on Discharge in Electrolyte Solution Under Same Ultrasonic Power

Discharge experiments are carried out under the same ultrasonic power of 300 W in six kinds of electrolyte solutions with different electrolyte concentrations ranging from 5 to 60 g electrolyte/200 mL deionized water. Taking NaCl as an example, the detailed operations are listed as follows:

Firstly, 5, 15, 30, and 60 g of NaCl powder are weighed and put into four volumetric beakers, respectively, and the deionized water is added into beakers to the 200 mL mark. A glass stirring rod is used to stir the electrolyte solution till the NaCl is completely dissolved.

The prepared nickel metal strips in groups of two are hung on the beaker edges with the longer part of the strip inside the beaker and fixed by an ordinary ticket clip to ensure

that the nickel metal strip stays still. The same measures are taken for the other three beakers. After that, the four beakers are fixed inside the ultrasonic cleaning equipment via cable ties.

Spent BAK 18650-2150 Mah LIBs with an initial voltage of 3.8 V are used for the discharge experiment, as shown in Figure 1a. The batteries are installed in four battery boxes, and a multifunction electricity meter is used to measure the voltage of batteries at both ends to make sure they have the same voltage of approximately 3.8 V before the discharge, as shown in Figure 1b. After the ultrasonic power is adjusted to 300 W, the ultrasonic cleaning equipment is turned on. An appropriate time interval is selected to record the residual voltage data points based on the voltage change rate. In this experiment, the residual voltage is generally recorded every two minutes in the initial stage, and after the discharge speed shows significant reduction, it gradually transits to five-minute and thirty-minute intervals.
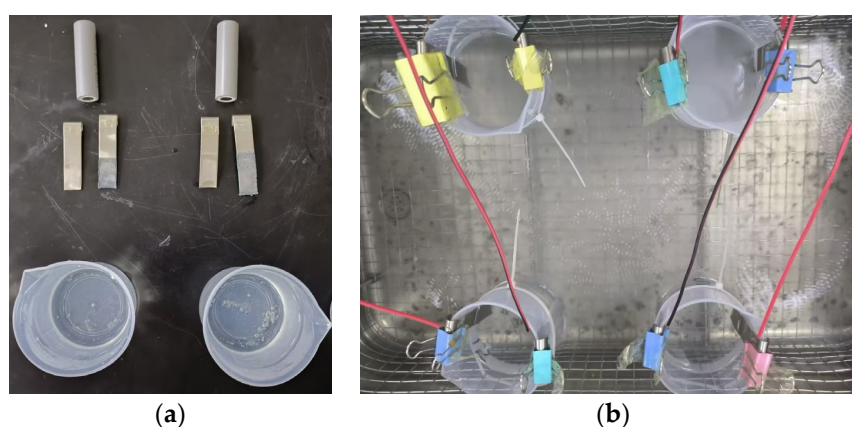

(**a**)	(**b**)

Figure 1. Spent LIB batteries used for the discharge (**a**) and discharge experimental setup are fixed inside the ultrasonic cleaning equipment (**b**).

After discharge, the experimental components are disassembled. Small amounts of both the supernatant and sediment of each solution are collected using a rubber dropper and stored in plastic centrifuge tubes for further analysis.

The same operation procedures are repeated for other samples to complete the scheduled experiments.

2.4. Pretreatment and Discharge Efficiency Calculation

A big nickel metal piece is cut into several rectangular strips with a length of about 11 cm. A small part of one end of the rectangular piece is bent into an appropriate arc which is beneficial for hanging, and the length of the end is about a quarter of the total length of the rectangular piece.

Firstly, the sheath with a length of roughly 1 cm is cut off at both ends of the wire to expose the copper wire core. One end of the two wires is wrapped around the metal fixtures on both sides of the battery box, and the other end of the two wires is bound to the center of two nickel metal strips using sticky tapes.

The *DE* is defined as the difference (V) between the initial voltage (V) and residual voltage (V) divided by the initial voltage (V), as shown in Equation (1).

$$\text{Discharge Efficiency } (DE) = \frac{\text{Initial Voltage} - \text{Residual Voltage}}{\text{Initial Voltage}} \times 100\% \qquad (1)$$

2.5. Effects of Different Ultrasonic Powers in Same Electrolyte Solution

Previous experiments have demonstrated that NaCl and KCl solutions with varying electrolyte concentrations play a crucial role in the discharge process. In contrast, four other electrolytes (Na_2SO_4, HCOONa, CH_3COONa, $(CH_3COO)_2Zn$) which have minimal impact on the discharge are also selected. To further investigate their effects under different ultrasonic conditions, electrolyte solutions are prepared, and discharge experiments are conducted at various ultrasonic power levels ranging from 100 to 500 W while maintaining a constant electrolyte mass concentration.

Taking the ultrasonic power of 100 W as an example, 20 g of each electrolyte sample is weighed and placed into four well-labeled beakers. Then, 180 mL of deionized water is measured using a graduated cylinder and transferred to the beaker via a rubber dropper. A glass stirring rod is then used to mix the solution until the electrolyte is completely dissolved.

This procedure is repeated for consistency. Once the batteries are installed and their status is confirmed, the ultrasonic power is adjusted to 100 W, and the ultrasonic cleaning equipment is started. The remaining voltage data are recorded at appropriate time intervals throughout the experiment.

After the discharge, the experimental components are disassembled, and small amounts of both the supernatant and sediment of each solution are collected and stored in plastic centrifuge tubes for further analysis.

The entire experiment is then repeated under the ultrasonic powers of 300 and 500 W to examine the effects of increased ultrasonic intensity on the discharge process.

3. Results and Discussion

3.1. Experimental Phenomenon

During the discharge, it can be clearly observed that there is a large amount of green sediment in NaCl and KCl solutions with different electrolyte concentrations, as shown in Figure 2. The Na_2SO_4 solution appears light green, and there is a small amount of sediment produced. The amount of sediment is positively correlated with the electrolyte concentration.
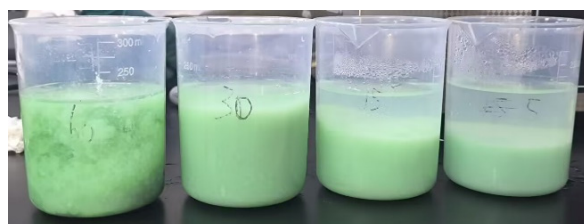

Figure 2. The KCl solutions appeared green at different levels and sediments appeared in the beaker.

The nickel strips show an obvious corrosion phenomenon during the discharge process in NaCl and KCl solution, which is manifested as a complete fracture of the part immersed in the solution or a large-scale irregular defect. The defective part is always stained with green sediment, as shown in Figure 3. The nickel strip in the Na_2SO_4 solution is slightly corroded and stained with a small amount of green sediment in the electrolyte solution with high Na_2SO_4 concentration.

Figure 3. The corroded nickel strip after the discharge in KCl solution. From left to right: 60, 30, 15, and 5 g/200 mL deionized water.

For the discharge in other electrolyte solutions, the nickel strip remains almost intact, and the solution remains almost transparent. A certain number of bubbles are generated in the organic salt solution with a high concentration (30 g/200 mL deionized water and above) at the bottom of the beaker, as shown in Figure 4. The nickel strip in the $(CH_3COO)_2Zn$ solution is stained with blue sediment.

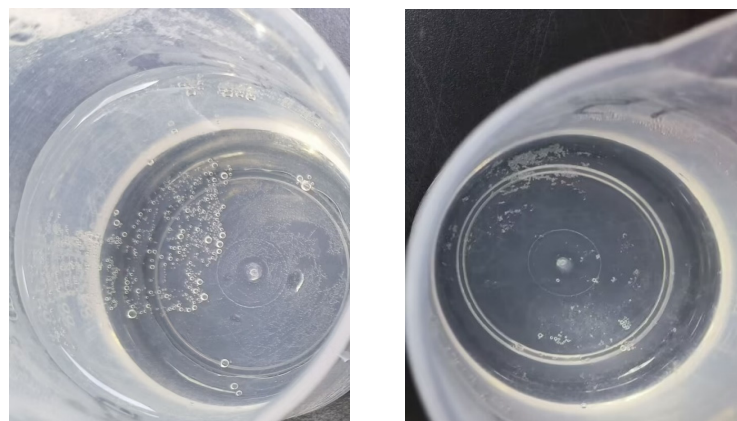**Figure 4.** Bubbles are generated at the bottom of beakers with the organic electrolyte (left: CH_3COONa, right: $(CH_3COO)_2Zn$) solution at a high concentration (30 g/200 mL deionized water and above).

The suspension in each beaker is filtered using a circulating water vacuum pump and labeled well. The filtration cake is dried in an oven at 60 °C overnight and then weighed for further analysis.

3.2. Effect of Electrolyte Concentration Without Ultrasonic Treatment

The discharge experiments are carried out in Na_2SO_4 solution with various mass concentrations, and the residual voltage of spent LIBs over time during the discharge is displayed in Figure 5. The recorded voltage of spent LIBs decreases from 3.80 to 3.68 V, 3.78 to 3.60 V, 3.77 to 3.56 V, and 3.79 to 3.59 V as the Na_2SO_4 mass concentration increases from 5, 15, 30, to 60 g per 200 mL deionized water, respectively. According to Equation (1), the calculated *DE*s are 3.2, 4.8, 5.6, and 5.3%, respectively. This trend indicates that, in general, the overall *DE* gradually increases when increasing the Na_2SO_4 concentration, reaching a maximum of 5.6% at 30 g/200 mL of deionized water. However, a further increase in concentration to 60 g/200 mL deionized water resulted in a slight decline in *DE*. This reduction in *DE* at higher electrolyte concentrations may be attributed to the formation of sediment deposits, as shown in Figure 2, which block the active reaction sites on the

nickel metal strips, thereby limiting the *DE*. Therefore, an optimal Na_2SO_4 solution of 30 g/200 mL deionized water is recommended for effective discharge.
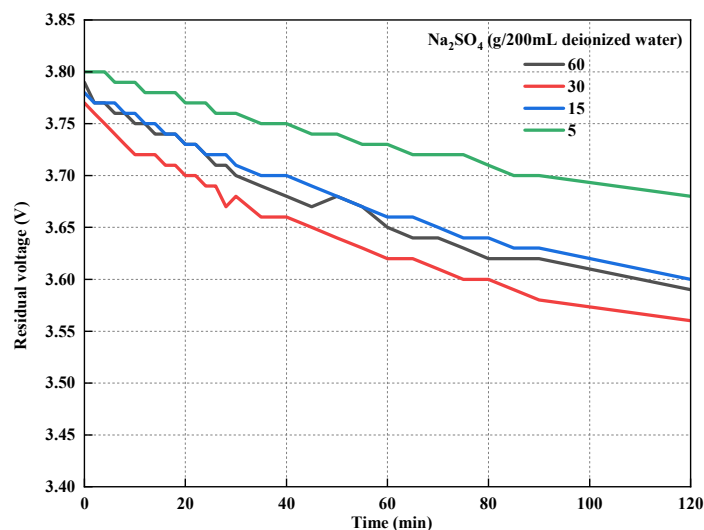

Figure 5. Residual voltage of spent LIBs with time during the discharge in Na_2SO_4 solution with various mass concentrations.

Jiang et al. [37] compared the discharge effects of cylindrical LIBs with an initial voltage of about 3.8 V in Na_2SO_4 solutions with various mass concentrations (5% and 10%) and observed similar discharge trends across both experimental conditions. After 30 h of discharge, the battery voltage then dropped below 1 V. Similarly, Su et al. [36] studied the charge of spent LIBs in Na_2SO_4 solutions without ultrasonic assistance or additional discharge media. Their results showed that, in the absence of an electrolyte, the battery voltage remained nearly unchanged. However, when discharged in Na_2SO_4 solution with various mass concentrations of 50%, 75%, and saturation levels for 46 h, the batter voltage remained around 1 V. Further discharge in 25 wt.% Na_2SO_4 solution for 54 h reduced the voltage to 1 V. Stirring can mitigate the adverse effects of precipitation during discharged in Na_2SO_4 solutions. Under stirring conditions (600 rpm), complete discharge was achieved in 5 wt.% Na_2SO_4 solution within 9.3 h; while in 10 wt.% Na_2SO_4 solution, the discharge was completed in just 3.1 h. This is a notable improvement compared to unstirred NaCl solution where the discharge process takes longer time resulting in a lower *DE* [28].

The discharge experiments are carried out in HCOONa solution with various mass concentrations, and the residual voltage of spent LIBs over time during the discharge is displayed in Figure 6. The recorded voltage of spent LIBs decreases from 3.80 to 3.66 V, 3.78 to 3.58 V, 3.79 to 3.56 V, and 3.76 to 3.41 V as the HCOONa mass concentration increases from 5, 15, 30, to 60 g per 200 mL deionized water, respectively. According to Equation (1), the calculated *DE*s are 3.7, 5.3, 6.1, and 9.3%, respectively, indicating a progressive increase in *DE* as the HCOONa concentration increases. This trend is likely due to the increased concentration of conductive ions in the electrolyte solution, which accelerates the discharge reaction and enhances the *DE*.

The discharge experiments are carried out in CH_3COONa solution with various mass concentrations, and the residual voltage of spent LIBs over time during the discharge is displayed in Figure 7. The recorded voltage of spent LIBs decreases from 3.80 to 3.67 V, 3.75 to 3.53 V, 3.77 to 3.51 V, and 3.77 to 3.47 V as the CH_3COONa concentration increases from 5, 15, 30, to 60 g per 200 mL deionized water, respectively. According to Equation (1), the calculated *DE*s are 3.4, 5.9, 6.9, and 8.0%, respectively. This trend indicates that the *DE* gradually increases as the CH_3COONa concentration increases. The likely reason for this

improvement is that increasing the CH_3COONa concentration enhances the concentration of conductive ions in the electrolyte solution accelerating the discharge reaction of spent LIBs and thereby improving the *DE*.
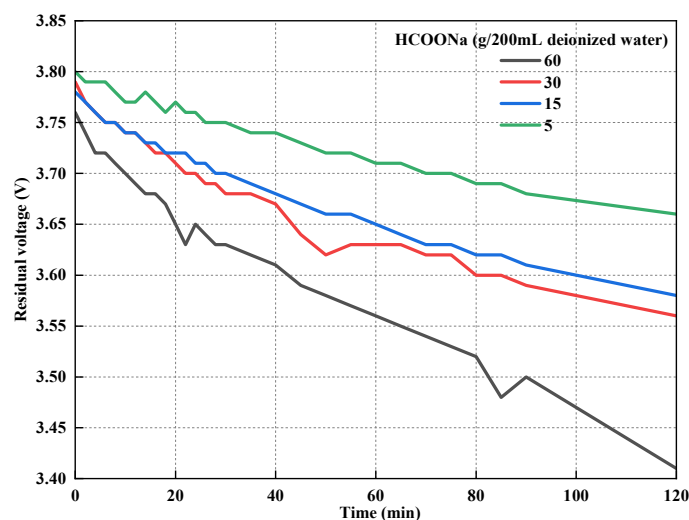

Figure 6. Residual voltage of spent LIBs with time during the discharge in HCOONa solution with various mass concentrations.
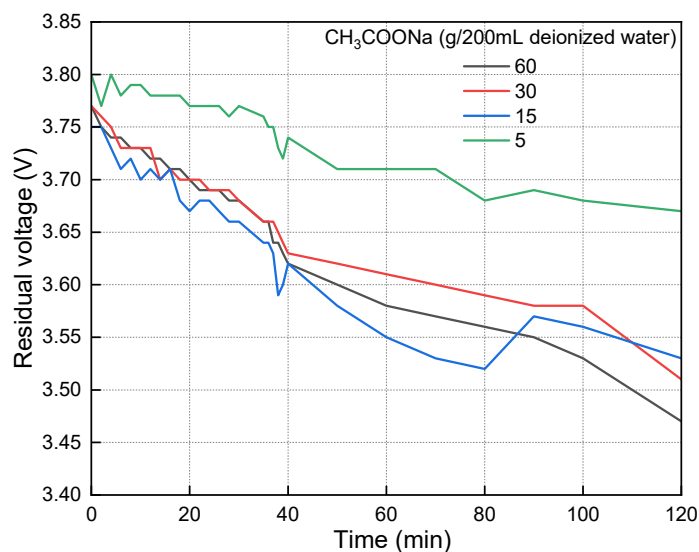

Figure 7. Residual voltage of spent LIBs with time during the discharge in CH_3COONa solution with various mass concentrations.

The discharge experiments are carried out in $(CH_3COO)_2Zn$ solution with various mass concentrations, and the residual voltage of spent LIBs over time during the discharge is displayed in Figure 8. The recorded voltage of spent LIBs decreases from 3.81 to 3.76 V, 3.81 to 3.72 V, 3.80 to 3.74 V, and 3.78 to 3.70 V as the $(CH_3COO)_2Zn$ mass concentration increases from 5, 15, 30, to 60 g/200 mL deionized water, respectively. According to Equation (1), the calculated *DE*s are 1.3, 2.4, 1.6, and 2.1%, respectively. These results indicate that the highest *DE* is achieved at a $(CH_3COO)_2Zn$ concentration of 15 g/200 mL deionized water, while the lowest occurred at 5 g/200 mL deionized water. Fang et al. [35] investigated the use of acetate as a discharge medium for chemically discharging the 18650 cylindrical LIB and found no corrosion on the battery shell in the acetate solution. This phenomenon can be attributed to a unique electrolysis reaction of acetate during the discharge, known as the Kolbe reaction [38]. The reaction intermediates form a protective

layer on the anode surface, inhibiting the oxidation-reduction reactions at the anode and effectively preventing battery shell corrosion during the discharge.
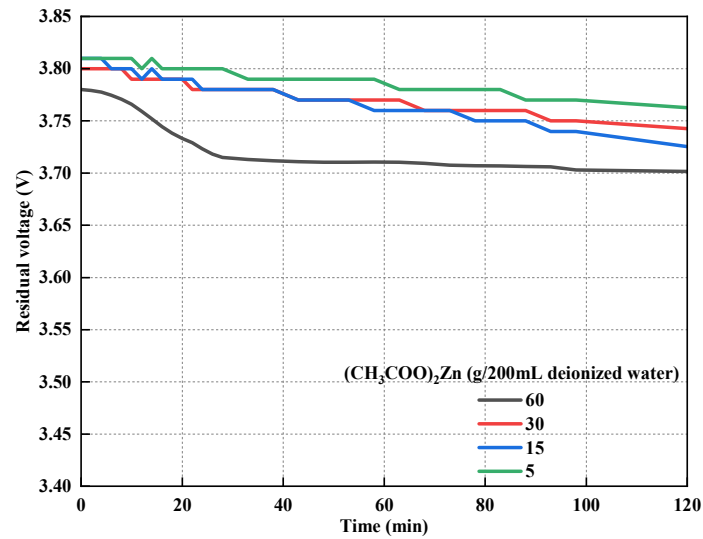

Figure 8. Residual voltage of spent LIBs with time during the discharge in $(CH_3COO)_2Zn$ solution with various mass concentrations.

The discharge experiments are carried out in NaCl solution with various mass concentrations, and the residual voltage of spent LIBs with time during the discharge process is displayed in Figure 9. The recorded voltage of spent LIBs decreases from 3.75 to 3.54 V, 3.75 to 3.47 V, 3.70 to 1.36 V, and 3.42 to 1.33 V as the NaCl mass concentration increases from 5, 15, 30, to 60 g/200 mL deionized water, respectively. According to Equation (1), the calculated *DE*s are 5.6, 7.5, 63.2, and 61.1%, respectively. These results indicate that, in general, the overall *DE* gradually increases as the NaCl concentration increases, reaching a maximum of 63.2% at 30 g/200 mL of deionized water. However, when the NaCl concentration increases to 60 g/200 mL of deionized water, the *DE* slightly decreases. Considering various factors, a NaCl solution with a concentration of 30 g/200 mL of deionized water is deemed the most suitable for discharge.
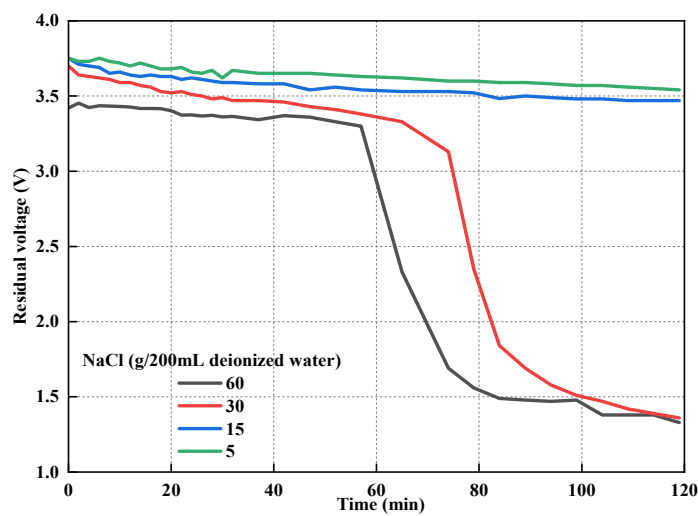

Figure 9. Residual voltage of spent LIBs with time during the discharge in NaCl solution with various mass concentrations.

To further assess the effectiveness of NaCl solution as a chemical discharge medium, experiments were conducted with varying NaCl concentrations to meet specific experimental objectives. Li et al. [18] reported that the *DE* obtained in 10 wt.% NaCl solution is higher than that generated from NaCl solutions with other concentrations while posing no environmental harm. Lu et al. [39] found that, under similar experimental conditions, the electrolyte inside the electrode shell leaked, leading to the formation of HF gas, which could significantly impact subsequent recycling, while in 1 wt.% NaCl solution, the battery could be safely discharged to a voltage below the safe threshold voltage without causing shell damage. Additionally, Su et al. [36] found the electrolyte leakage could react with water generating hazardous gases such as HF in their research. As shown in Figure 4, a considered number of bubbles formed in a high-concentration organic salt solution (30 g/200 mL deionized water and above). This bubble formation is attributed to the electrolytic decomposition of water, producing H_2 and O_2 during battery discharge. Besides, organic salts such as acetate, may undergo chemical reactions, generating CO_2 during the discharge [29,31,35].

The discharge experiments are carried out in KCl solution with various mass concentrations, and the residual voltage of spent LIBs over time during the discharge is displayed in Figure 10. The recorded voltage of spent LIBs decreases from 3.82 to 3.58 V, 3.83 to 1.89 V, 3.82 to 1.34 V, and 3.83 to 1.46 Vas the KCl mass concentration increases from 5, 15, 30, to 60 g per 200 mL deionized water, respectively. According to Equation (1), the calculated *DE*s are 6.3, 50.7, 64.9, and 61.9%, respectively. These results indicate that the overall *DE* gradually increases with rising the KCl concentration, reaching a maximum of 64.9% at 30 g/200 mL of deionized water. However, when the KCl concentration increases to 60 g/200 mL of deionized water, the *DE* slightly decreases. Considering various factors, a KCl solution with a concentration of 30 g/200 mL deionized water is the most suitable for the discharge process. Chen et al. [31] also conducted battery discharge experiments using 10 wt.% KCl solution and found that the remaining power of the battery was effectively consumed, further confirming the effectiveness of KCl solution as a discharge medium.
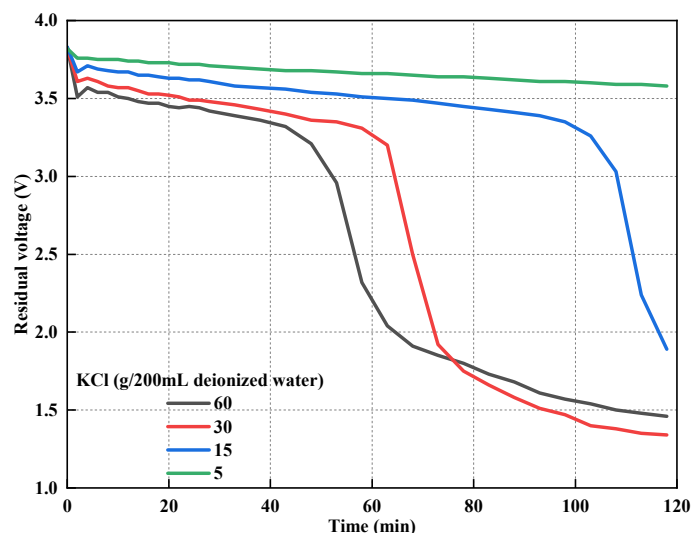

Figure 10. Residual voltage of spent LIBs with time during the discharge in KCl solution with various mass concentrations.

3.3. Effects of Ultrasonic Power

The discharge experiments are carried out under an ultrasonic power of 100 W in various electrolyte solutions with a mass concentration of 10 wt.%. The residual voltage of spent LIBs over time under these experimental conditions is displayed in Figure 11a. As

can be seen from Figure 11a, the residual voltage decreases from 3.8 to 3.65 V in Na_2SO_4 solution, 3.8 to 3.67 V in HCOONa solution, 3.81 to 3.65 V in CH_3COONa solution, and 3.82 to 3.72 V in $(CH_3COO)_2Zn$ solution. Based on Equation (1), the calculated *DE*s from the discharge in Na_2SO_4, HCOONa, CH_3COONa, and $(CH_3COO)_2Zn$ solutions are 3.9, 3.4, 4.2, and 2.6%, respectively. These results indicate the highest *DE* is obtained from the discharge in the CH_3COONa solution, while the discharge in the $(CH_3COO)_2Zn$ solution results in the lowest *DE*.
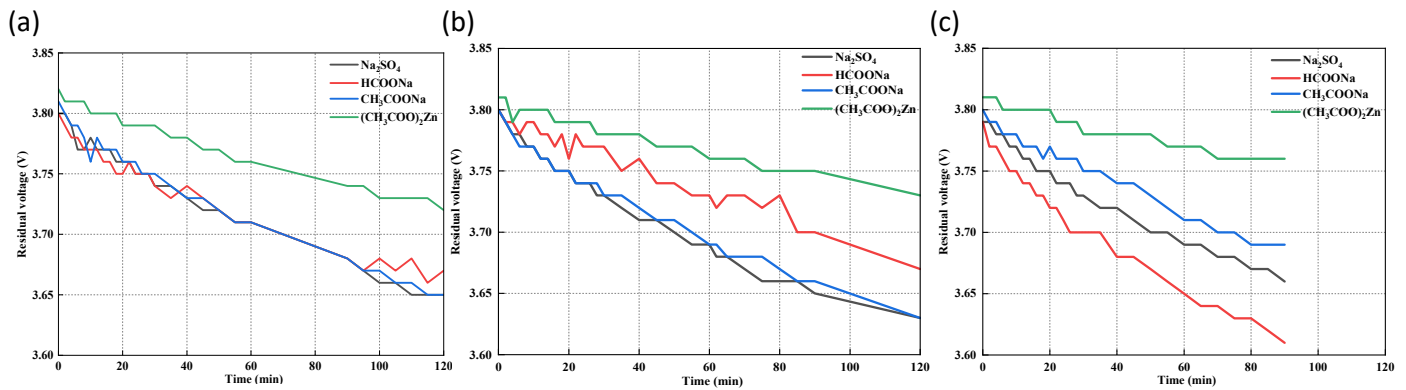

Figure 11. Residual voltage of spent LIBs with time during the discharge assisted with ultrasonic power of 100 W (**a**), 300 W (**b**), and 500 W (**c**) in various electrolyte solutions with a mass concentration of 10 wt.%.

The discharge experiments are carried out under an ultrasonic power of 300 W in various electrolyte solutions with a mass concentration of 10 wt.%. The residual voltage of spent LIBs over time under these experimental conditions is displayed in Figure 11b. As can be seen from Figure 11b, the residual voltage decreases from 3.8 to 3.63 V in Na_2SO_4, 3.8 to 3.67 V in HCOONa solution, 3.8 to 3.63 V in CH_3COONa solution, and 3.81 to 3.73 V in $(CH_3COO)_2Zn$ solution. Based on Equation (1), the generated *DE*s from the discharge in Na_2SO_4, HCOONa, CH_3COONa, and $(CH_3COO)_2Zn$ solutions are 4.5, 3.4, 4.5, and 2.1%, respectively. These results indicate the *DE*s obtained from the Na_2SO_4 and CH_3COONa solutions are the same and rank the highest under the abovementioned experimental conditions, while the lowest *DE* is generated from the discharge in $(CH_3COO)_2Zn$ solution.

The discharge experiments are carried out under an ultrasonic power of 500 W in various electrolyte solutions with a mass concentration of 10 wt.%. The residual voltage of spent LIBs over time under these experimental conditions is displayed in Figure 11c. As can be seen from Figure 11c, the residual voltage decreases from 3.79 to 3.66 V in Na_2SO_4 solution, 3.79 to 3.61 V in HCOONa solution, 3.8 to 3.69 V in CH_3COONa solution, and 3.81 to 3.76 V in $(CH_3COO)_2Zn$ solution. Based on Equation (1), the generated *DE*s from the discharge processes in Na_2SO_4, HCOONa, CH_3COONa, and $(CH_3COO)_2Zn$ solutions are 3.4, 4.7, 2.9, and 1.3%, respectively. These results indicate that the highest *DE* is obtained from the discharge in the HCOONa solution, while the discharge in the $(CH_3COO)_2Zn$ solution results in the lowest *DE*.

By combining Figure 11a–c, Figure 12 is generated. As can be seen from Figure 12, the *DE* obtained from the discharge in Na_2SO_4 solution (DE_{Na2SO4}) initially increases from 3.9 to 4.5% as the ultrasonic power rises from 100 to 300 W but then decreases to 3.4% at 500 W, with the mass concentration remaining 10 wt.%. In HCOONa solution (10 wt.%), the generated *DE* remains constant at 3.4% under ultrasonic powers of 100 W and 300 W but increases to 4.7% at 500 W with other experimental parameters unchanged. In CH_3COONa solution, the *DE* shows a slight increase from 4.2 to 4.5% before decreasing to 2.9%, while in $(CH_3COO)_2Zn$ keep the *DE* continuously decreases from 2.6 to 1.3%.

The positive effect of ultrasonic waves on the battery discharge can be attributed to their ability to accelerate solvent dissolution and generate numerous cavitation bubbles. When these bubbles collapse, the resulting shock waves help dislodge salt deposits near the electrodes and minimize the formation of precipitation, thereby enhancing battery discharge performance in electrolyte solutions [29].
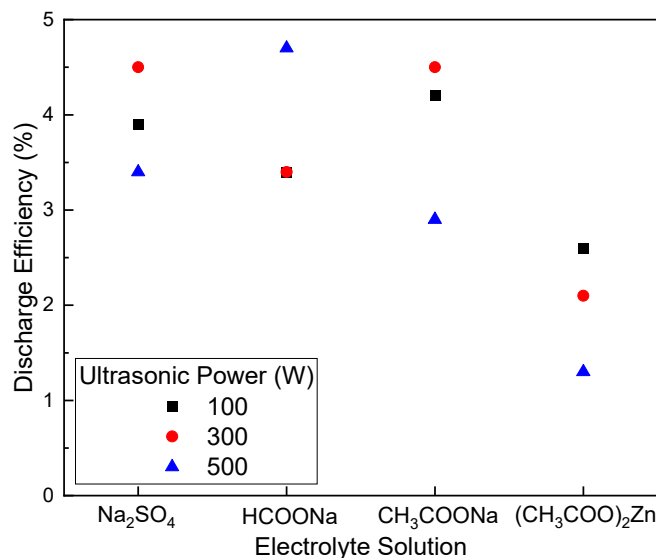

Figure 12. *DE*s generated from the discharge under various ultrasonic powers in different electrolyte solutions with the same electrolyte mass concentration of 10 wt.%.

3.4. XRF Analysis

The suspended liquid after discharge was characterized by XRF analysis to investigate the elements and compound composition in the suspension after discharge, and the results are displayed in Figure 13. From Figure 13(a1,a2), the proportion of each element in the suspension of discharged spent LIBs is as follows: 33 wt.% Ni, 32 wt.% Cl, and 29 wt.% K; while the content of Ca, Si, Fe, Mg, Al, Ti, and S is almost zero. It can be seen from Figure 13(b1,b2) that the mixture is composed of 37 wt.% NiO, 32 wt.% K_2O, and 30 wt.% Cl, respectively; while the contents of SiO_2, CaO, Fe_2O_3, MgO, Al_2O_3, TiO_2, and SO_3 are almost zero. The highest mass concentrations of elements and complexes after discharge are Ni and NiO, respectively, indicating severe corrosion of the nickel metal strip in NaCl and KCl solutions, as shown in Figure 3. When a chlorine salt solution is used as the discharge medium, it enables efficient discharge but also leads to severe casing corrosion. This occurs due to the pitting corrosion effect of chloride ions, which chemically "attack" the battery shell during discharge and accelerate galvanic corrosion. As a result, the battery experiences significant deterioration throughout the discharge process [31,40]. However, in other electrolyte solutions (Na_2SO_4, HCOONa, CH_3COONa, and $(CH_3COO)_2Zn$), the nickel metal strips did not suffer severe corrosion.
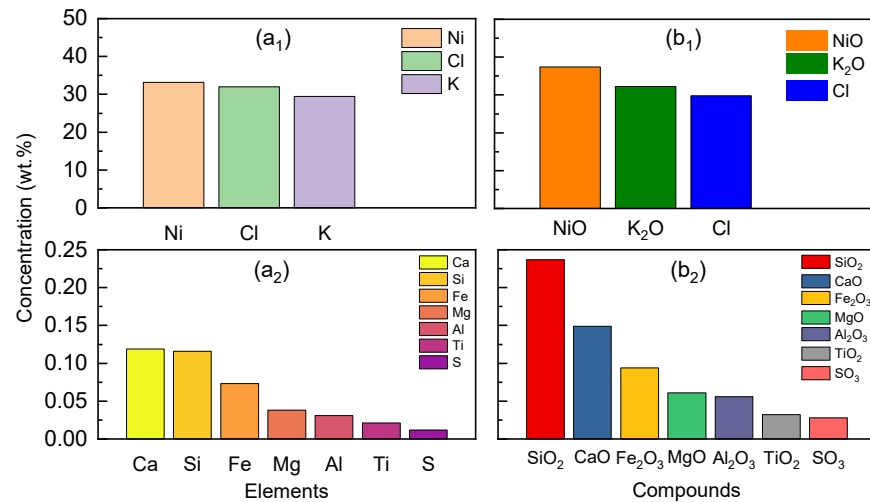
Figure 13. XRF analysis: elemental (a_1,a_2) and compound (b_1,b_2) analysis of the suspension after the discharge.

3.5. pH Analysis

3.5.1. pH of Electrolyte Solution After Discharge with Different Ultrasonic Powers

The pH measurements of the electrolyte solution after the discharge with different ultrasonic powers were performed and the results are presented in Figure 14. As can be seen from Figure 14, there are no significant changes in the pH value of various electrolyte solutions when different ultrasonic powers (100 or 500 W) are applied. After discharge, the pH value of the 10 wt.% Na_2SO_4 solution is 4, whereas the pH values of HCOONa, CH_3COONa, and $(CH_3COO)_2Zn$ solutions of the same concentration are 8, 7, and 4, respectively. These results indicate that the application of ultrasonic power does not change the pH of electrolyte solutions after discharge.
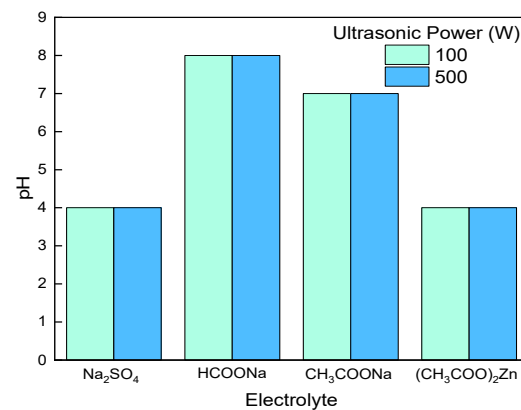

Figure 14. pH values of electrolyte solutions after discharge under ultrasonic powers of 100 and 500 W.

3.5.2. pH of Electrolyte Solution with Different Mass Concentrations After Discharge

Figure 15 presents the pH values of Na_2SO_4, HCOONa, $(HCOO)_2Zn$, NaCl, and KCl solutions with different mass concentrations after discharge. As shown in Figure 15, for Na_2SO_4, HCOONa, and $(HCOO)_2Zn$ solutions at various electrolyte concentrations (60, 30, 15, and 5 g/200 mL deionized water), there are no changes in their pH values after discharge, which remained 4, 8, and 4, respectively. In contrast, the pH values of NaCl solutions with different mass concentrations (60, 30, 15, and 5 g/200 mL deionized water) are 13, 11, 10, and 8, respectively; while the pH values of KCl solutions at the same mass concentrations are 13, 11, 9, and 7, respectively. Additionally, when the *DE* is very low,

there is minimal change in the pH value. These results indicate that the mass concentrations of Na$_2$SO$_4$, HCOONa, and (HCOO)$_2$Zn do not affect the pH of the electrolyte solution after discharge. However, the mass concentrations of NaCl and KCl solutions significantly influence the pH of the electrolyte solution after discharge.
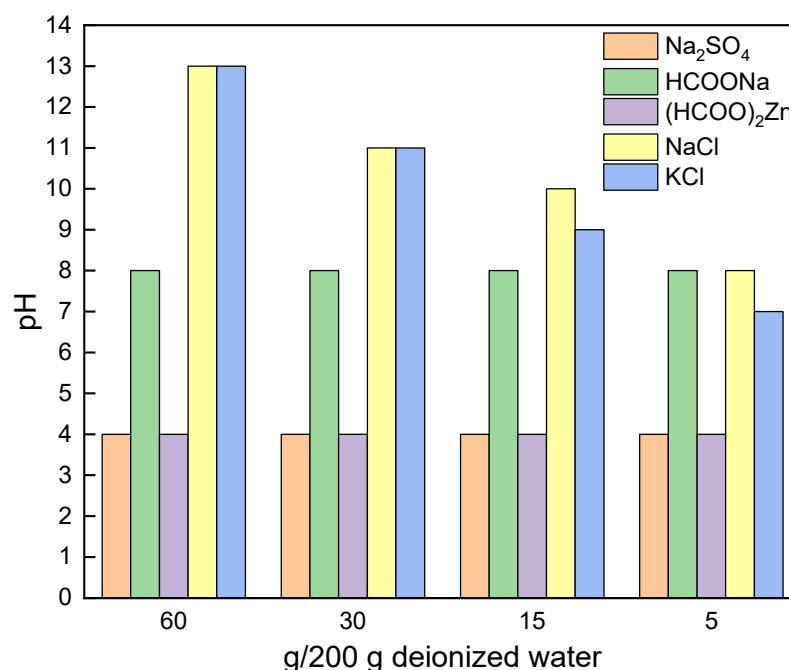

Figure 15. pH values of Na$_2$SO$_4$, HCOONa, (HCOO)$_2$Zn, NaCl, and KCl solutions with different mass concentrations after discharge.

4. Conclusions

The spent LIBs are discharged in various electrolyte solutions with different mass concentrations, as well as in the same electrolyte solution with varying ultrasonic powers. Characterizations, including pH measurement and XRF analysis, are employed to evaluate the *DE* of spent LIBs. After a thorough assessment, the following conclusions were drawn:(1) The *DE*s obtained from experiments using NaCl and KCl solutions are significantly improved under ultrasonic treatment, while the *DE*s generated from using organic electrolyte solutions, primarily containing formate and acetate, remained generally lower than the ideal *DE*. (2) Under the same ultrasonic power, the highest *DE* (64.9%) is achieved using 30 g KCl/200 mL deionized water. However, the pH values of NaCl and KCl solutions changed, leading to significant corrosion of nickel metal strips. (3) In the same electrolyte solution, the highest *DE* of 4.7% was obtained from discharging in a 10 wt.% HCOONa solution under 500 W ultrasonic power. In this case, the pH value of the solution and the nickel metal strip remained unchanged after discharge.

Based on these conclusions, future research will be focus on optimizing the *DE* using various electrolyte solutions under appropriate ultrasonic power. This approach aims to facilitate the economical and environmentally friendly recycling of spent LIBs.

References

1. Wang, S.; Yu, J. A Comparative Life Cycle Assessment on Lithium-Ion Battery: Case Study on Electric Vehicle Battery in China Considering Battery Evolution. *Waste Manag. Res.* **2021**, *39*, 156–164. [CrossRef]
2. Hossain, R.; Sarkar, M.; Sahajwalla, V. Technological Options and Design Evolution for Recycling Spent Lithium-ion Batteries: Impact, Challenges, and Opportunities. *WIREs Energy Environ.* **2023**, *12*, e481. [CrossRef]
3. Wang, Y.; Diao, W.; Fan, C.; Wu, X.; Zhang, J. Benign Recycling of Spent Batteries towards All-Solid-State Lithium Batteries. *Chem.—Eur. J.* **2019**, *25*, 8975–8981. [CrossRef]
4. Niu, B.; Xiao, J.; Xu, Z. Recycling Spent $LiCoO_2$ Battery as a High-efficient Lithium-doped Graphitic Carbon Nitride/Co_3O_4 Composite Photocatalyst and Its Synergistic Photocatalytic Mechanism. *Energy Environ. Mater.* **2023**, *6*, e12312. [CrossRef]
5. Meshram, P.; Pandey, B.D.; Mankhand, T.R. Recovery of Valuable Metals from Cathodic Active Material of Spent Lithium Ion Batteries: Leaching and Kinetic Aspects. *Waste Manag.* **2015**, *45*, 306–313. [CrossRef]
6. Xiao, J.; Li, J.; Xu, Z. Novel Approach for in Situ Recovery of Lithium Carbonate from Spent Lithium Ion Batteries Using Vacuum Metallurgy. *Environ. Sci. Technol.* **2017**, *51*, 11960–11966. [CrossRef]
7. Golmohammadzadeh, R.; Faraji, F.; Rashchi, F. Recovery of Lithium and Cobalt from Spent Lithium Ion Batteries (LIBs) Using Organic Acids as Leaching Reagents: A Review. *Resour. Conserv. Recycl.* **2018**, *136*, 418–435. [CrossRef]
8. Xiao, J.; Li, J.; Xu, Z. Challenges to Future Development of Spent Lithium Ion Batteries Recovery from Environmental and Technological Perspectives. *Environ. Sci. Technol.* **2020**, *54*, 9–25. [CrossRef]
9. Duan, X.; Zhu, W.; Ruan, Z.; Xie, M.; Chen, J.; Ren, X. Recycling of Lithium Batteries—A Review. *Energies* **2022**, *15*, 1611. [CrossRef]
10. Tong, Z.; Ren, X.; Ni, M.; Bu, X.; Dong, L. Review of Ultrasound-Assisted Recycling and Utilization of Cathode Materials from Spent Lithium-Ion Batteries: State-of-the-Art and Outlook. *Energy Fuels* **2023**, *37*, 14574–14588. [CrossRef]
11. Guo, B.; Liu, X.; He, R.; Gao, X.; Yan, X.; Yang, S. Advances on Mechanism of Degradation and Thermal Runaway of Lithium-Ion Batteries. *Chin. J. Rare Met.* **2024**, *48*, 225–239. [CrossRef]
12. Zhang, H.; Bai, T.; Cheng, J.; Ji, F.; Zeng, Z.; Li, Y.; Zhang, C.; Wang, J.; Xia, W.; Ci, N.; et al. Unlocking the Decomposition Limitations of the $Li_2C_2O_4$ for Highly Efficient Cathode Prelithiations. *Adv. Powder Mater.* **2024**, *3*, 100215. [CrossRef]
13. Zhong, W.; Tao, J.; Chen, Y.; White, R.G.; Zhang, L.; Li, J.; Huang, Z.; Lin, Y. Unraveling the Evolution of Cathode–Solid Electrolyte Interface Using Operando X-Ray Photoelectron Spectroscopy. *Adv. Powder Mater.* **2024**, *3*, 100184. [CrossRef]
14. Fujita, T.; Chen, H.; Wang, K.; He, C.; Wang, Y.; Dodbiba, G.; Wei, Y. Reduction, reuse and recycle of spent Li-ion batteries for automobiles:A review. *Int. J. Miner. Metall. Mater.* **2021**, *28*, 179–192. [CrossRef]
15. Zhang, G.; Yuan, X.; He, Y.; Wang, H.; Zhang, T.; Xie, W. Recent Advances in Pretreating Technology for Recycling Valuable Metals from Spent Lithium-Ion Batteries. *J. Hazard. Mater.* **2021**, *406*, 124332. [CrossRef]
16. Zhong, X.; Liu, W.; Han, J.; Jiao, F.; Qin, W.; Liu, T. Pretreatment for the Recovery of Spent Lithium Ion Batteries: Theoretical and Practical Aspects. *J. Clean. Prod.* **2020**, *263*, 121439. [CrossRef]
17. Punt, T.; Bradshaw, S.M.; Van Wyk, P.; Akdogan, G. The Efficiency of Black Mass Preparation by Discharge and Alkaline Leaching for LIB Recycling. *Minerals* **2022**, *12*, 753. [CrossRef]
18. Li, J.; Wang, G.; Xu, Z. Generation and Detection of Metal Ions and Volatile Organic Compounds (VOCs) Emissions from the Pretreatment Processes for Recycling Spent Lithium-Ion Batteries. *Waste Manag.* **2016**, *52*, 221–227. [CrossRef]
19. Zhang, T.; He, Y.; Ge, L.; Fu, R.; Zhang, X.; Huang, Y. Characteristics of Wet and Dry Crushing Methods in the Recycling Process of Spent Lithium-Ion Batteries. *J. Power Sources* **2013**, *240*, 766–771. [CrossRef]
20. Wang, D.; Li, X.; Chen, Z.; Wang, S.; Wang, Y.; Liu, W.; Li, W.; Xue, R.; Liu, C.T. Susceptibility of Chloride Ion Concentration, Temperature, and Surface Roughness on Pitting Corrosion of CoCrFeNi Medium-entropy Alloy. *Mater. Corros.* **2022**, *73*, 106–115. [CrossRef]
21. Ali, H.; Khan, H.A.; Pecht, M. Preprocessing of Spent Lithium-Ion Batteries for Recycling: Need, Methods, and Trends. *Renew. Sustain. Energy Rev.* **2022**, *168*, 112809. [CrossRef]
22. Ren, X.; Tong, Z.; Dai, Y.; Ma, G.; Lv, Z.; Bu, X.; Bilal, M.; Vakylabad, A.B.; Hassanzadeh, A. Effects of Mechanical Stirring and Ultrasound Treatment on the Separation of Graphite Electrode Materials from Copper Foils of Spent LIBs: A Comparative Study. *Separations* **2023**, *10*, 246. [CrossRef]

23. Zhang, G.; He, Y.; Wang, H.; Feng, Y.; Xie, W.; Zhu, X. Application of Mechanical Crushing Combined with Pyrolysis-Enhanced Flotation Technology to Recover Graphite and LiCoO 2 from Spent Lithium-Ion Batteries. *J. Clean. Prod.* **2019**, *231*, 1418–1427. [CrossRef]

24. Tong, Z.; Dong, L.; Wang, X.; Bu, X. Enhancement Mechanism of the Difference of Hydrophobicity between Anode and Cathode Active Materials from Spent Lithium-Ion Battery Using Plasma Modification. *ACS Sustain. Chem. Eng.* **2024**, *12*, 8541–8551. [CrossRef]

25. Wang, B.; Lin, X.-Y.; Tang, Y.; Wang, Q.; Leung, M.K.H.; Lu, X.-Y. Recycling LiCoO 2 with Methanesulfonic Acid for Regeneration of Lithium-Ion Battery Electrode Materials. *J. Power Sources* **2019**, *436*, 226828. [CrossRef]

26. Qiu, X.; Tian, Y.; Deng, W.; Li, F.; Hu, J.; Deng, W.; Chen, J.; Zou, G.; Hou, H.; Yang, Y.; et al. Coupling Regeneration Strategy of Lithium-Ion Electrode Materials Turned with Naphthalenedisulfonic Acid. *Waste Manag.* **2021**, *136*, 1–10. [CrossRef] [PubMed]

27. Lee, H.; Kim, Y.-T.; Lee, S.-W. Optimization of the Electrochemical Discharge of Spent Li-Ion Batteries from Electric Vehicles for Direct Recycling. *Energies* **2023**, *16*, 2759. [CrossRef]

28. Ojanen, S.; Lundström, M.; Santasalo-Aarnio, A.; Serna-Guerrero, R. Challenging the Concept of Electrochemical Discharge Using Salt Solutions for Lithium-Ion Batteries Recycling. *Waste Manag.* **2018**, *76*, 242–249. [CrossRef] [PubMed]

29. Torabian, M.M.; Jafari, M.; Bazargan, A. Discharge of Lithium-Ion Batteries in Salt Solutions for Safer Storage, Transport, and Resource Recovery. *Waste Manag. Res.* **2022**, *40*, 402–409. [CrossRef] [PubMed]

30. Juarez-Robles, D.; Vyas, A.A.; Fear, C.; Jeevarajan, J.A.; Mukherjee, P.P. Overdischarge and Aging Analytics of Li-Ion Cells. *J. Electrochem. Soc.* **2020**, *167*, 090558. [CrossRef]

31. Chen, X.; Hua, W.; Yuan, L.; Ji, S.; Wang, S.; Yan, S. Evolution Fate of Battery Chemistry during Efficient Discharging Processing of Spent Lithium-Ion Batteries. *Waste Manag.* **2023**, *170*, 278–286. [CrossRef]

32. Yao, L.P.; Zeng, Q.; Qi, T.; Li, J. An Environmentally Friendly Discharge Technology to Pretreat Spent Lithium-Ion Batteries. *J. Clean. Prod.* **2020**, *245*, 118820. [CrossRef]

33. Su, Y.; Lu, S.; Zhou, H.; Yang, W. Research on safe discharge of used power lithium-ion batteries. *Compr. Util. Resour. China* **2020**, *38*, 40–42+52.

34. Paulino, J.F.; Busnardo, N.G.; Afonso, J.C. Recovery of Valuable Elements from Spent Li-Batteries. *J. Hazard. Mater.* **2008**, *150*, 843–849. [CrossRef] [PubMed]

35. Fang, Z.; Duan, Q.; Peng, Q.; Wei, Z.; Cao, H.; Sun, J.; Wang, Q. Comparative Study of Chemical Discharge Strategy to Pretreat Spent Lithium-Ion Batteries for Safe, Efficient, and Environmentally Friendly Recycling. *J. Clean. Prod.* **2022**, *359*, 132116. [CrossRef]

36. Su, Y.; Lu, S.; Zhou, H.; Yang, W. Experimental study on chemical discharge of used lithium-ion batteries. *Min. Metall.* **2021**, *30*, 90–94+106.

37. Jiang, L.; Zheng, W.; Zhang, G.; Zhang, Z.; Zhang, K.; Xu, K.; Lai, Y.; Yang, J. Research on green discharge technology for the pretreatment of waste lithium-ion batteries. *J. Cent. South Univ. (Nat. Sci. Ed.)* **2023**, *54*, 684–693.

38. Holzhäuser, F.J.; Mensah, J.B.; Palkovits, R. (Non-)Kolbe Electrolysis in Biomass Valorization—A Discussion of Potential Applications. *Green Chem.* **2020**, *22*, 286–301. [CrossRef]

39. Lu, M.; Zhang, H.; Wang, B.; Zheng, X.; Dai, C. The Re-Synthesis of LiCoO2 from Spent Lithium Ion Batteries Separated by Vacuum-Assisted Heat-Treating Method. *Int. J. Electrochem. Sci.* **2013**, *8*, 8201–8209. [CrossRef]

40. Xiao, J.; Guo, J.; Zhan, L.; Xu, Z. A Cleaner Approach to the Discharge Process of Spent Lithium Ion Batteries in Different Solutions. *J. Clean. Prod.* **2020**, *255*, 120064. [CrossRef]